



**Acoustics'08
Paris**
June 29-July 4, 2008

www.acoustics08-paris.org

Semi-analytical modelling of plate flexural waves generated by laser-initiated air shock waves

Vasil Georgiev^a, Victor Krylov^a, Qin Qin^b and Keith Attenborough^{c,b}

^aLoughborough University, Department of Aeronautical and Automotive Engineering, Ashby Road, LE11 3TU Loughborough, UK

^bUniversity of Hull, Department of Engineering, Cottingham Road, HU6 7RX Hull, UK

^cOpen University, Department of Design, Development, Materials and Environment, Walton Hall, MK7 6AA Milton Keynes, UK

v.v.krylov@lboro.ac.uk

The paper describes the results of the semi-analytical modelling of the interaction of laser-initiated air shock waves with an infinite elastic plate. The impact of the incident shock wave on the plate has been approximated by an equivalent cylindrically diverging surface force resulting from the combined surface pressure of the incident and reflected shock waves. This force has been then represented in the wavenumber-frequency domain by means of Hankel and Fourier transforms which have been carried out numerically - and the problem has been solved using the Green's function method applied to an infinite plate. The resulting frequency spectra and time shapes of the generated flexural wave pulses have been calculated for different values of laser pulse energy and for different heights of the laser beam focusing above the plate surface. The obtained theoretical results have been compared with the results of the reduced-scale model experiments on shock wave interaction with the ground in which large plastic and wooden plates have been used to represent the ground surface. The comparison shows that the obtained semi-analytical results are in good agreement with the experimental ones.

1 Introduction

It is well known that controlled explosions taking place above ground surface during military tests generate shock waves in the air as well as strong vibrations in the ground. It is convenient and much less expensive to study the associated sound and vibration phenomena using reduced-scale laboratory simulations, with a laser as a source of air shock waves interacting with large elastic plates modelling the ground [1,2]. Earlier, a semi-analytical model of interaction of air shock waves with an elastic half space has been suggested to describe generation of Rayleigh surface waves by electric spark discharge near the surface[3].

The aim of the present paper is to extend the semi-analytical approach [3] to describe the interaction of laser-initiated air shock waves with an infinite elastic plate resulting in generation of flexural waves in the plate (see also Ref. 4). The impact of the incident shock wave is approximated by an equivalent cylindrically diverging surface force resulting from the surface pressure of the incident and reflected shock waves. The expressions are

$$P^{sh}(r, t) = P^{sh}(r)H\left(t - \int_0^r \frac{dr'}{v^{sh}(r')}\right) \exp\left[-\left(t - \int_0^r \frac{dr'}{v^{sh}(r')}\right)\left(\varepsilon \int_0^r \frac{dr'}{v^{sh}(r')}\right)^{-1}\right], \quad (1)$$

Here $H(t)$ is a Heaviside step function, $v^{sh}(r)$ and $P^{sh}(r)$ are particle velocity and pressure in the front of a shock wave [5] and $\varepsilon = 0.05$ is a constant controlling the duration of the pressure pulse:

$$v^{sh}(r) = \frac{2}{5} \zeta_0^{5/2} \left(\frac{E}{\rho_0}\right)^{1/2} r^{-3/2}, \quad (2)$$

$$P^{sh}(r) = \left(\frac{2}{5}\right)^2 \frac{2\zeta_0^5}{\gamma+1} E r^{-3}, \quad (3)$$

E is the energy instantly released in the origin of the shock wave, ρ_0 is the mass density of the air, $\gamma \approx 1.41$ is the Poisson adiabat, and $\zeta_0 \approx 0.93$ is the dimensionless parameter characterizing the self-similar motion of the wave front [5].

As a result of interaction of the shock wave with an infinite plate, a considerable part of the incident wave energy is reflected back into the air, whereas the remainder is transformed into the energy of flexural plate vibrations. To evaluate the air pressure acting on the plate surface, the

constructed to describe pressure pulses of the air shock wave and the resulting equivalent surface force as a function of time and horizontal distance from the epicentre. The problem is then solved using the Green's function method applied to an infinite plate. The resulting frequency spectra and time histories of the generated flexural waves are calculated for different values of height of the laser-generated spark above the plate surface. The obtained theoretical results for time histories and frequency spectra of generated flexural waves are compared with the results of the reduced-scale model experiments on shock wave interaction with a large plastic plate.

2 Theoretical background

2.1 Equivalent surface force induced by a strong shock wave

According to Ref. 3, the pressure in a strong spherically diverging air shock wave can be approximated by the following simple analytical expression:

latter can be approximated as absolutely rigid. In this case, the surface pressure can be considered as the sum of the incident and reflected pressures. Using the usual linear acoustic reflection coefficient for a rigid surface (equal to 1), the resulting surface pressure can be expressed simply as twice the pressure in the incident wave [3]. Thus, the equivalent normal surface force per unit area F_n^{sh} created by the shock wave can be expressed using Eqns (1) - (3) as

$$F_n^{sh}(t, \rho) = 2P^{sh}(r)H[t - t_0^{sh}] \exp\{-[t - t_0^{sh}] / \varepsilon t_0^{sh}\}, \quad (4)$$

$$\text{where } t_0^{sh} = \left(\frac{r}{\zeta_0}\right)^{5/2} \left(\frac{\rho_0}{E}\right)^{1/2}.$$

In Eqn (4), the distance r from the origin of laser-induced acoustic shock to a point of observation on the surface is equal to $\sqrt{\rho^2 + h^2}$ (see Fig. 1).

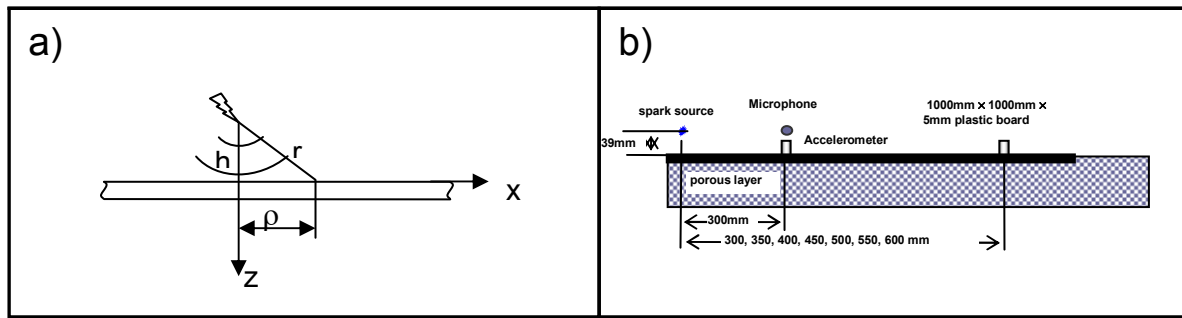


Fig. 1 Interaction of laser-initiated air shock waves with a plate: (a) – geometry of the problem, (b) – experimental scheme.

For further analysis, the frequency spectrum of the normal force $F_n^{sh}(t, \rho)$ is required:

$$F_n^{sh}(\omega, \rho) = \frac{1}{2\pi} \int_{-\infty}^{+\infty} F_n^{sh}(t, \rho) \exp(i\omega t) dt \quad (5)$$

Substituting Eqn (4) into Eqn (5), this frequency spectrum can be expressed as follows:

$$F_n^{sh}(\omega, \rho) = \frac{P^{sh}(r)}{\pi} \frac{\epsilon t_0^{sh}}{1 - i\omega \epsilon t_0^{sh}} \exp(i\omega t_0^{sh}) \quad (6)$$

2.2 Modified equivalent surface force

In the previous section, the equivalent surface force (Eqn (4)) has been specified using Eqns (1)-(3) valid for strong shock waves in air. The time history of the air pressure pulse calculated according to Eqns (1)-(3) can be seen in Fig. 2 (a). Note however that the values of height h in the

model experiments [1,2,4] were generally rather large, and an initially strong air shock wave, when it reaches the plate for such values of h is gradually transformed into a weak shock wave. A more detailed theoretical description and measurements of pressure pulses induced by such a weak shock wave show that, when the shock front approaches a given point, the pressure initially undergoes a discontinuous jump above the atmospheric pressure. Then it decreases below the atmospheric pressure (positive and negative phases), and finally returns to its initial value [5].

In the light of the above, the expression (1) can be modified to model wave pulses of weak shock waves, which is more adequate for the description of the above-mentioned model experiments. For this purpose, an additional exponential term to describe the negative pressure phase can be added to Eqn (1). The air pressure can then be expressed as follows (see also Fig. 2 (b)):

$$P^{sh}(r, t) = P^{sh}(r) \left\{ H(t - t_0^{sh}) \left[1.2 \exp\left(-\frac{t - t_0^{sh}}{\epsilon t_0^{sh}}\right) - 0.2 \right] - H(t - t_0^{sh} 3.5) \left[1.2 \exp\left(-\frac{t - t_0^{sh}}{\epsilon t_0^{sh}} \frac{0.36}{\epsilon t_0^{sh}}\right) - 0.2 \right] \right\} \quad (7)$$

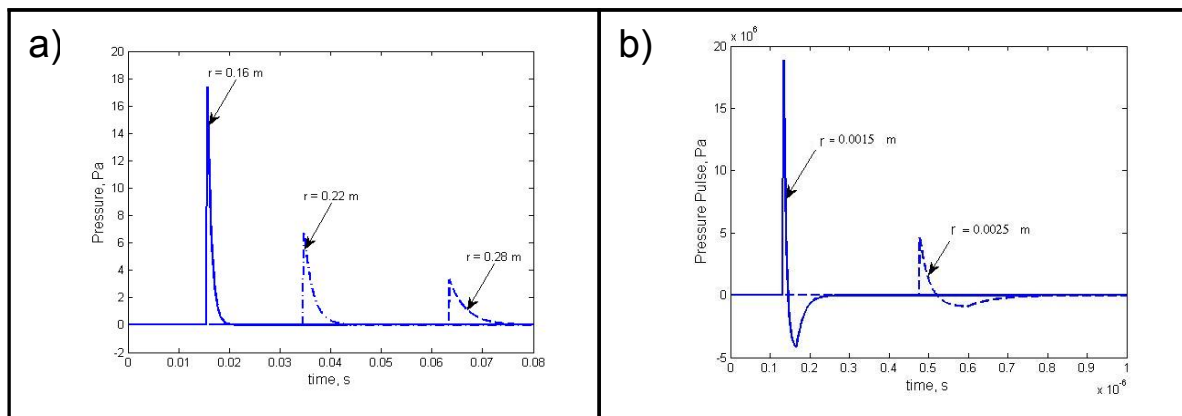


Fig. 2 Air pressure pulses calculated according to Eqn (1) - (a) and to Eqn (7) - (b).

Using the above-mentioned modified expression for air pressure (Eqn (7)) and the acoustic approximation for the reflection coefficient, the equivalent surface force can be expressed as:

$$F_n^{sh}(\omega, \rho) = \frac{P^{sh}(r)}{\pi} \left\{ \frac{1.2 \epsilon t_0^{sh}}{1 - i\omega \epsilon t_0^{sh}} \exp(i\omega t_0^{sh}) - \frac{0.2}{i\omega} [\exp(i\omega t_0^{sh} 3.5) - \exp(i\omega t_0^{sh})] - \frac{1.2 \epsilon t_0^{sh}}{0.36 - i\omega \epsilon t_0^{sh}} \exp\left(-\frac{0.9}{\epsilon} + i\omega t_0^{sh} 3.5\right) \right\}. \quad (8)$$

$$F_n^{sh}(r, t) = 2P^{sh}(r, t),$$

Using Fourier transform, the frequency spectrum of the above function can be expressed as follows:

Note that the above expressions for the equivalent surface force (Eqns (6) and (8)) still have been constructed using Eqns (2) and (3) for velocity and pressure of a strong air shock wave [5]. However, for distances r that are large enough, say $r > r_0$, where r_0 is the distance at which the particle velocity at a shock front becomes equal to the speed of sound, the above-mentioned expressions for surface forces are no longer valid. In the case under consideration, the air particle velocity and pressure beyond the distance $r_0 = 0.0084$ m (defined from Eqn (2) for $v_0 = 340$ m/s and $E = 0.8$ J is the laser energy per pulse), have to be calculated using the characteristics of a normal acoustic wave propagating with the speed of sound v_0 . The wave pressure in this case is inversely proportional to the distance: $P(r) = A/r$, where the constant A should be

determined by equalising the air pressure in the shock wave to the acoustic wave pressure at $r = r_0$. Moreover, the time duration of a pressure pulse in a strong shock wave increases proportionally to the distance from the epicentre, whereas in a normal acoustic wave this duration is constant. Thus, the time duration of the pressure pulses at distance $r = r_0$ should be equalized as well. For an acoustic wave, Eqns (2) and (3) should be replaced by

$$v^{ac} = v_0 = 340 \text{ m/s},$$

$$P^{ac}(r) = \left(\frac{2}{5}\right)^2 \frac{2\zeta_0^5}{\gamma + 1} \frac{E}{r_0^2 r} \quad (9)$$

Using the above equations, one can obtain the following expression valid for $r > r_0$:

$$P^{ac}(r, t) = P^{ac}(r) \left\{ H(t - t_0^{ac}) \left[1.2 \exp\left(-\frac{(t - t_0^{ac})}{\varepsilon t_0^{sh}(r_0)}\right) - 0.2 \right] - H(t - t_0^{ac} - 2.5t_0^{sh}(r_0)) \left[1.2 \exp\left(-\frac{(t - t_0^{ac})}{\varepsilon t_0^{sh}(r_0)}\right) - 0.2 \right] \right\}, \quad (10)$$

where $t_0^{ac} = t_0^{sh}(r_0) + \frac{r - r_0}{v_0}$. In Eqn (10), we have modified some of the fitting coefficients used in our previous calculations [4] to match the observed parameters of the transformed acoustic wave pulses more precisely.

Using again the linear acoustics approximation for the reflection coefficient, the equivalent normal surface force for $r > r_0$ can be written down as the doubled incident pressure, and the frequency spectrum of the equivalent surface force can be expressed as:

$$F_n^{ac}(\omega, \rho) = \frac{P^{ac}(r)}{\pi} \left\{ \begin{aligned} & \frac{1.2\varepsilon t_0^{sh}(r_0)}{1 - i\omega\varepsilon t_0^{sh}(r_0)} \exp(i\omega t_0^{ac}) - \frac{0.2}{i\omega} [\exp(i\omega(t_0^{ac} + t_0^{sh}(r_0))) - \exp(i\omega t_0^{ac})] - \\ & \left[-\frac{1.2\varepsilon t_0^{sh}(r_0)}{0.36 - i\omega\varepsilon t_0^{sh}(r_0)} \exp\left(-\frac{0.9}{\varepsilon} + i\omega(t_0^{ac} + 2.5t_0^{sh}(r_0))\right) \right] \end{aligned} \right\} \quad (11)$$

2.3 Generation of flexural waves in a plate by incident shock waves

Since the problem under consideration is axisymmetric, the flexural response of the infinite plate to the spectral component of the applied normal force $F_n(x, y, \omega)$ due to the incident air shock wave can be described using the Green's function method [6] (see Ref. [4] for more detail). Introducing cylindrical coordinates with the origin at the epicentre, one can write down the applied normal force as:

$$F_n(\omega, \rho) = \begin{cases} F_n^{sh}, & 0 < r < r_0 \\ F_n^{ac}, & r > r_0 \end{cases}. \quad (12)$$

$$F_n(\omega, k) = \int_0^{\rho_0} F_n^{sh}(\omega, \rho) \rho J_0(k\rho) d\rho + \int_{\rho_0}^{\infty} F_n^{ac}(\omega, \rho) \rho J_0(k\rho) d\rho \quad (14)$$

The inverse Hankel transform describes the plate response to the acoustic shock in the space-frequency domain. Expressing the Bessel function in the inverse Hankel transform in terms of Hankel functions, the resulting bending displacement can be written as:

$$w(\omega, \rho) = \frac{1}{2D} \int_{-\infty}^{\infty} \frac{F_n(\omega, k) k H_0^{(1)}(k\rho) dk}{k^4 - k_f^4} \quad (15)$$

This yields the following expression for bending displacements of the generated flexural waves in the wavenumber-frequency domain [6]:

$$\tilde{w}(\omega, k) = \frac{F_n(\omega, k)}{D(k^4 - k_f^4)}. \quad (13)$$

Here $D = \tilde{E}d^3/12(1 - \nu^2)$ is the bending stiffness of the plate, \tilde{E} is the Young's modulus, d is the plate thickness, ν is the Poisson's ratio, $k_f = (\rho_s h \omega^2 / D)^{1/4}$ is the plate flexural wavenumber, and $F_n(\omega, k)$ is the Hankel transform of Eqn (12) which should be calculated numerically:

The integral in Eqn (15) can be evaluated in the complex k -plane using the method of residues:

$$w(\omega, \rho) = 2\pi i \left(\frac{1}{2D} \frac{F_n(\omega, k_f) k_f H_0^{(1)}(k_f \rho)}{4k_f^3} \right), \quad (16)$$

where the term in brackets represents the residue at $k = k_f$. Using the well-known asymptotic formula for the Hankel

function at $k_f \rho \gg 1$, the expression for plate vertical

displacement can be finally written as follows:

$$w(\omega, \rho) = \frac{iF_n(\omega, k_f)}{4\omega^{5/4} \rho_s^{5/8} d^{5/8} D^{3/8}} \sqrt{\frac{2\pi}{\rho}} \exp(ik_f \rho - i\pi/4). \quad (17)$$

Combined with the harmonic time factor $e^{-i\omega t}$, this expression represents a cylindrical flexural wave propagating from the epicenter of the acoustic shock. Obviously, the vertical components of plate particle velocity and acceleration can be obtained from Eqn (17) as:

$$\dot{w}(\omega, \rho) = -i\omega w(\omega, \rho); \quad \ddot{w}(\omega, \rho) = -\omega^2 w(\omega, \rho).$$

The time history of the displacement can then be calculated from Eqn (17) using the inverse Fourier transform:

$$w(t, \rho) = \int_{-\infty}^{\infty} w(\omega, \rho) e^{-i\omega t} d\omega. \quad (18)$$

3 Experimental investigations

The rig used for the model experiments is shown in Fig.1 (b). Sparks were generated by a Q-switch Surelite III-10 Nd: YAG laser with a 1064 nm wavelength and the energy of 0.8 J per pulse. For the measurements of flexural vibrations, a DJB A/20 accelerometer with the mass 18 g, sensitivity 35 pC/g and resonant frequency 28 kHz was

used. The plate was made of laminated plastic material. Its horizontal dimensions and thickness were $1 \times 1 \text{ m}^2$ and 0.005 m respectively. Measurements were carried out for two heights of the laser generated spark over the plate surface: 0.039 m and 0.003 m. The accelerometer was placed at two distances from the epicentre: 0.3 m and 0.6 m. Further details about the laboratory equipment and test rig can be found in Refs 1 and 2.

4 Comparison of the theoretical and experimental results

In this section some of the results of theoretical modelling and experimental simulations are presented and compared (see Figs. 3 and 4). The material characteristics used in the analytical calculations are as follows: mass density $\rho_s = 900 \text{ kg/m}^3$, Young's modulus $\tilde{E} = 50.10^8 \text{ N/m}^2$, Poisson's ratio $\nu = 0.3$.

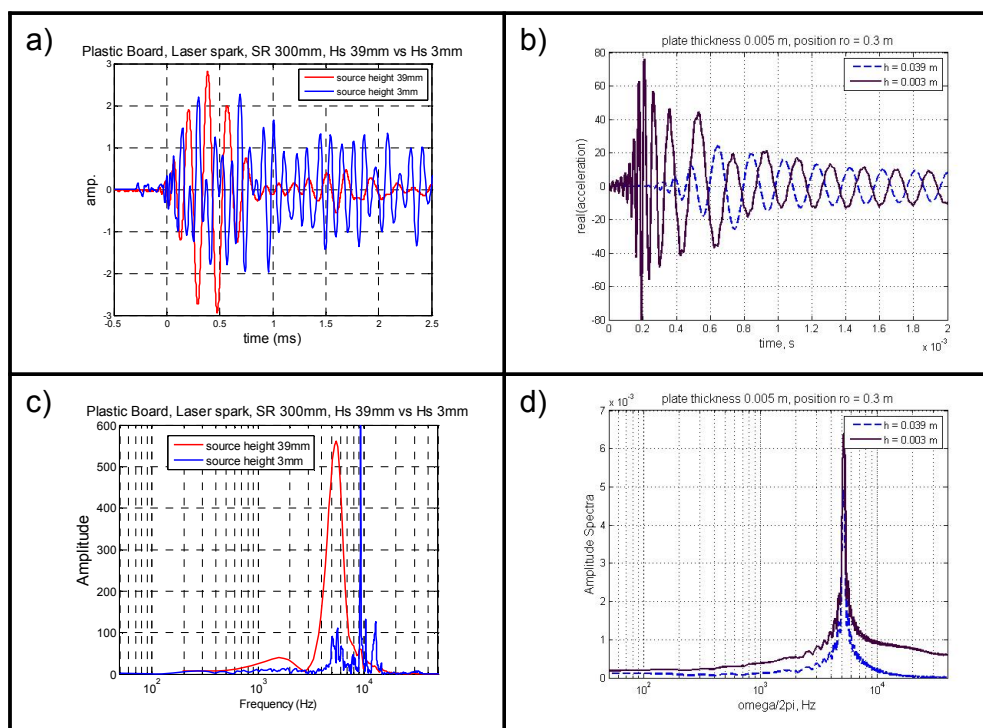


Fig. 3. Time history ((a), (b)) and amplitude spectra ((c), (d)) of the plate acceleration at distance 0.3 m away from the epicenter: measured ((a), (c)) and calculated ((b),(d)).

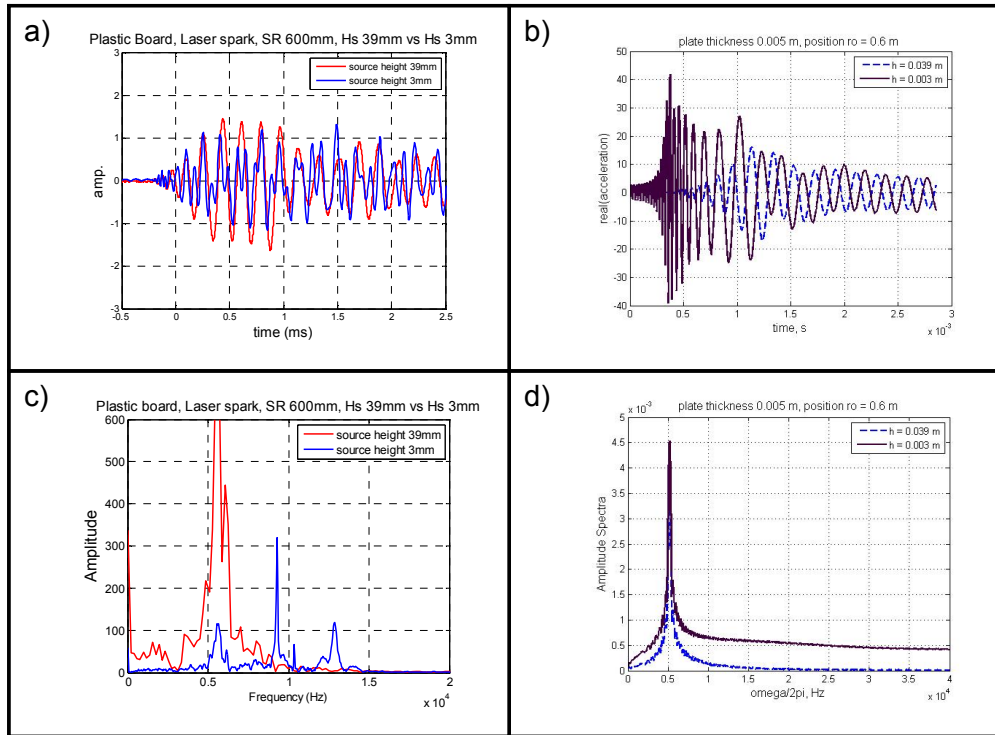


Fig. 4 Time history ((a), (b)) and amplitude spectra ((c), (d)) of the plate acceleration at distance 0.6 m away from the epicenter: measured ((a), (c)) and calculated ((b),(d)).

Figures 3 and 4 present the time histories and amplitude spectra of the plate normal acceleration at distances 0.3 m and 0.6 m away from the epicenter. The heights of the laser-generated spark above the plate are 0.039 m and 0.003 m. Both series of results, experimental and theoretical, show oscillations at frequency about 5 kHz. Apparently, this behaviour is due to a coincidence phenomenon, when sound waves incident on a plate have a trace wavelength matching to that of the plate bending wave.

The experimental frequency spectra at $h = 0.039$ m are broader than the theoretical ones. At $h = 0.003$ m some new peaks appear, whereas the theoretical prediction does not change significantly. The assumption has been made that these discrepancies could be attributed to non-linear reflection of shock waves. To check this assumption, the latter has been taken into account using the well-known analytical formula for shock wave reflection from a rigid surface [7]. It has been shown, however, that taking into account the non-linear reflection simply increases the amplitude and slightly changes the shape of the pressure pulse, mainly in the zone of strong shocks. Beyond the critical distance r_0 , the pressure associated with non-linear reflection is small in comparison with that due to linear one. As a result, the calculated time histories and amplitude spectra of the plate flexural waves do not differ significantly from those calculated using linear reflection.

5 Conclusions

A semi-analytical model of flexural wave generation in an infinite plate due to laser-initiated air shock waves has been developed. Analysis of the obtained results shows that the coincidence condition plays an important role in the observed phenomena, being responsible for harmonic oscillations around the coincidence frequency. The comparison of the calculated theoretical results with the

experimentally observed ones has shown reasonably good agreement. Some observed discrepancies may be caused by different wave generation and propagation mechanisms that require further attention.

Acknowledgments

The research reported here has been supported by EPSRC grant EP/E027121/1.

References

- [1] K. Attenborough and Q. Qin, Model experiments on shock wave interaction with the ground, Proceedings of the 19th ICA, Madrid, Spain, 2-7 September 2007 (on CD).
- [2] Q. Qin and K. Attenborough, Characteristics and application of laser-generated acoustic shock waves in air, *Applied Acoustics*, 65, 325-340 (2004).
- [3] V.V. Krylov, On the theory of surface acoustic wave generation by electric spark discharge, *J. Phys. D: Appl. Phys.*, 25, 155-161 (1992).
- [4] V.B. Georgiev, V.V. Krylov, Q. Qin and K. Attenborough, Generation of flexural waves in infinite plates by laser-initiated air shock waves, *Proc. IOA*, Vol. 30, Pt. 2, 147-154 (2008).
- [5] Y.B. Zel'dovich and Y.P. Raizer, *Physics of shock waves and high temperature hydrodynamic phenomena*, Vols 1, 2, New York: Academic Press (1966, 1967).
- [6] M.C. Junger and D. Feit, *Sound, structures and their interaction*, Cambridge: MIT Press (1972).
- [7] J.K. Wright, *Shock tubes*, New York: Wiley&Sons (1961).